Article

Greening and Browning Trends across Peru's Diverse Environments

Molly H. Polk [1],* , **Niti B. Mishra [2]** , **Kenneth R. Young [1]** and **Kumar Mainali [3,4]**

[1] Department of Geography and the Environment, University of Texas at Austin, Austin, TX 78712, USA; kryoung@austin.utexas.edu

[2] Department of Geography and Earth Science, University of Wisconsin, La Crosse, WI 54601, USA; nmishra@uwlax.edu

[3] Department of Biology, University of Maryland, College Park, MD 20742, USA; kpmainali@utexas.edu

[4] Conservation Innovation Center, Chesapeake Conservancy, Annapolis, MD 21401, USA

* Correspondence: mollypolk@utexas.edu

check for
updates

Abstract: If he were living today, Alexander von Humboldt would be using current technology to evaluate change in the Andes. Inspired by von Humboldt's scientific legacy and the 2019 celebrations of his influence, we utilize a Moderate Resolution Imaging Spectroradiometer (MODIS)time-series vegetation index to ask questions of landscape change. Specifically, we use an 18-year record of Normalized Difference Vegetation Index (NDVI) data as a proxy to evaluate landscape change in Peru, which is well known for its high biological and ecological diversity. Continent-level evaluations of Latin America have shown sites with a positive trend in NDVI, or "greening" and "browning", a negative trend in NDVI that suggests biophysical or human-caused reductions in vegetation. Our overall hypothesis was that the major biomes in Peru would show similar NDVI change patterns. To test our expectations, we analyzed the NDVI time-series with Thiel-Sen regression and evaluated Peru overall, by protected area status, by biome, and by biome and elevation. Across Peru overall, there was a general greening trend. By protected area status, surprisingly, the majority of greening occurred outside protected areas. The trends were different by biome, but there were hotspots of greening in the Amazon, Andean Highlands, and Drylands where greening dominated. In the Tropical Subtropical Dry Broadleaf Forest biome, greening and browning signals were mixed. Greening trends varied across the elevation gradient, switching from greening, to browning, and then back to greening as elevation increased. By biome and elevation, the results were variable. We further explored biome-specific drivers of greening and browning drawing on high-resolution imagery, the literature, and field expertise, much as we imagine von Humboldt might have approached similar questions of landscape dynamism.

Keywords: NDVI time-series; Thiel-Sen trend; greening; browning; Peru; landscape change; Latin America; MODIS

1. Introduction

Alexander von Humboldt explored the physical and human geography of the Americas from 1799 to 1804 [1–3]. He was masterful at observation, description, measurement, and synthesis. His documentation of plant distributions in the Andes Mountains [4,5] inspired ongoing studies of the effects of biophysical controls on vegetation [6] and his data gathering has literally been replicated to show upward species migrations and downward expansion of human-modified landscapes [7,8]. If he were living today, the Prussian polymath would be using current technology to evaluate change in the Andes. Inspired by his examples and the celebrations in 2019 of the anniversary of his birth and his

ongoing influence [9], we here utilize MODIS imagery to ask questions of landscape change occurring at a national scale in tropical South America. Humboldt famously evaluated change in reference to both human and biophysical factors in present-day Peru, Ecuador, Colombia, and Venezuela and elsewhere in Latin America [1–3], which is similar to how land change researchers frame their evaluations currently [10,11].

Specifically, we use an 18-year record of Normalized Difference Vegetation Index (NDVI) data as a proxy to evaluate land-cover change across the country of Peru, which is well known for its high biological and ecological diversity [12,13]. Other recent continent-level evaluations of Latin America have shown many sites with a positive trend in long term NDVI, known as "greening" [14,15]. The drivers of positive trends in vegetation greenness are often hypothesized to be global in extent, and due to greenhouse gases causing carbon dioxide fertilization and warming trends (although note that Zhu et al. use Leaf Area Index) [16]. Nevertheless, there are also situations where direct human action has increased vegetation cover, for example in the vast area afforested in China that represents part of that country's greening signal [17]. Thus, time-series vegetation indices such as NDVI offer means for assessing the relative contributions of atmospheric-mediated land-cover changes from those due to direct human actions in particular landscapes, typically at a more localized scale.

A decrease in NDVI trends over time, characterized as "browning," instead suggests biophysical or human-caused reductions in vegetation stature, biomass, or productivity. Such decreases have been detected in Australia, Africa, parts of South America, and in boreal forests [18,19]. In the Himalayas, Mishra and Mainali [20] showed that both greening and browning occurred, with the former often due to forest expansion, and the latter to its loss. They utilized a robust analysis of the NDVI time series with Thiel-Sen regression that we adapted for use here in our evaluation of change in Peru.

There are sharp environmental gradients in Peru, with climates on the coast that are hyper-arid and others in the Amazonian premontane forest that receive more than 6 m of annual rainfall [21,22]. Much biophysical change is due to elevation, with mountains frequently surpassing 5000 m and steep slopes forcing much turnover in species composition [23]. As a result, our null hypothesis was that the four major biomes in Peru would show similar NDVI change patterns, which would imply that atmospherically mediated global change was driving shifts across very different ecological conditions. Rejecting that overall hypothesis would instead suggest that biome-specific change processes are prevalent.

Aide et al. [15] isolated increases and decreases in woody plant biomass by elevation; their data for Peru showed most woody plant loss below 1500 m and most gain above. Similarly, we expected to find that elevation would be a significant control, and hypothesized finding similar results for land cover in general. Since 17.5% of Peru is located within areas formally designated for nature conservation [24], we expected that the greening would be especially related to conservation status, with browning more likely to be found in sites outside the national protected area (PA) system where human disturbance is more prevalent.

We present our findings here based on the trend analysis of 18 years of MODIS NDVI time-series imagery. We begin by clarifying how statistical significance was evaluated from the remotely sensed data. Next, we present NDVI trend results for Peru overall, by PA status, by biome, and by biome and elevation. In the discussion, we explore the biome-specific drivers of greening and browning by drawing on ancillary high-resolution imagery, the literature, and field expertise, much as we imagine von Humboldt might have approached similar country-scale questions.

2. Materials and Methods

2.1. Study Area

Located on the west coast of tropical South America between 0° S and 18° S, Peru is a global hotspot of diversity in terms of mammals, birds, amphibians, and plants [25–27]. Its tropical position and diverse topography (elevation ranges from sea level to 6786 m, the second highest peak on

the continent) explain the high biological diversity. With a total geographic area of 1,285,216 km², 87.4% is vegetated. The country's biodiversity can be organized into four biomes: Amazon, Andean Highlands, Drylands, and the Tropical Subtropical Dry Broadleaf Forest (TSDBF) (Figure 1). In the eastern lowlands, the Amazon is dominated by moist evergreen forests. The Andean Highlands consist of high elevation (>3000 m) grasslands, shrublands, remnant forests, glaciers, and bare rock. On the low elevation plain adjacent to the Pacific Ocean and the cold Humboldt Current, the Dry Coast is a hyper-arid biome mostly devoid of vegetation with the exception of fog-dependent plant communities (*lomas*) and groundwater-dependent plant communities. The TSDBF biome is ecotonal and is a confluence of biomes in northern South America, the Amazon, and the Andean Highlands. It is a heterogeneous mix of broadleaf deciduous forests and *páramo* (high elevation moist grasslands and shrublands) across a broad elevation gradient.
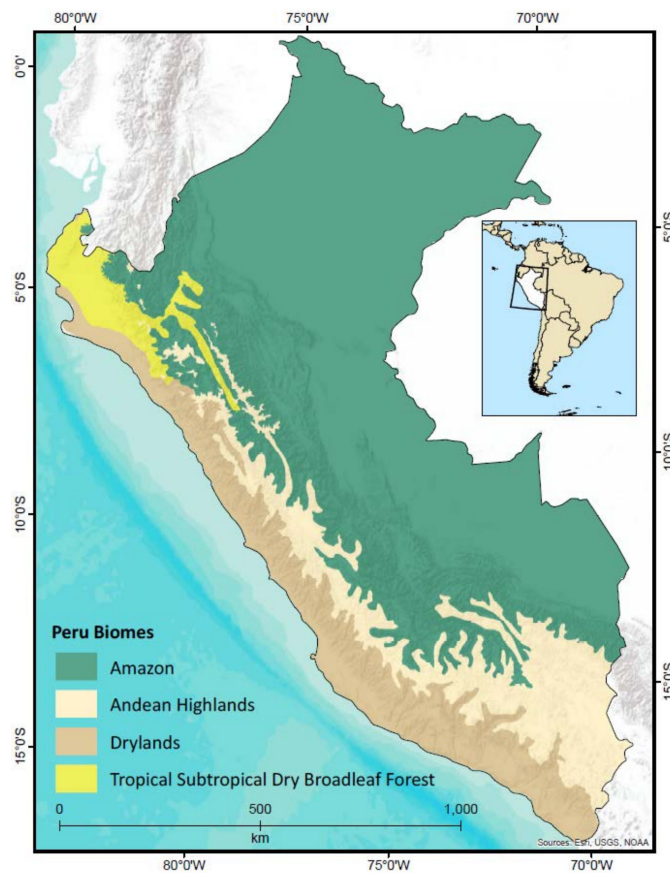

Figure 1. Peru and its four biomes. Inset map shows the location of Peru in South America.

Peru's climate is influenced by the Intertropical Convergence Zone (ITCZ), the El Niño Southern Oscillation (ENSO), prevailing easterlies, the orographic effect, and the Humboldt Current. The complex interactions among these features create wide variations in precipitation and temperatures. Precipitation patterns are especially variable seasonally and geographically, but broadly, precipitation ranges from essentially 0 mm/year along the central coast [28] up to 7000 mm/year at the Andean–Amazon interface [29]. Average temperatures are similarly variable spatiotemporally. For example, low temperatures in the high Andes can be below 0 °C. In the Drylands and in the Amazon, temperatures can reach 35 °C. Also relevant to greening, browning, and changing land use/land cover are economic activities. Peru's economy is dependent on extractive activities, including mined metals (copper, gold, zinc), hydrocarbons, agriculture, and fish products which are primarily destined for foreign markets.

2.2. Remote Sensing Pre-Processing

Methods are adapted from Mishra and Mainali [20], who evaluated greening trends across the Himalayas. After pre-processing was completed, the NDVI trend analysis was performed for several categories; the final phase was to explore causality (Figure 2). The remotely sensed data was the MODIS NDVI product (MOD13A3, Collection 6), a monthly 1-km spatial resolution dataset available from the National Aeronautics and Space Administration (NASA) (www.reveb.echo.nasa.gov). Compared to coarser spatial resolution but temporally longer time-series product (e.g., ~8 km spatial resolution of NOAA-AVHRR), this MODIS product represents a meaningful compromise of temporal length and spatial/temporal resolution and was preferred to account for the high spatial heterogeneity and functional diversity of vegetation in Peru. Unlike its predecessor (i.e., collection 5) which used composited daily data, the collection 6 of MOD13A2 uses pre-composited data which is atmospherically corrected with a modified compositing algorithm that aims at reducing the aerosol issues (minimizing the blue band). It is, however, QA driven and tries to constrain the view angle to minimize bidirectional reflectance distribution function effects [30].
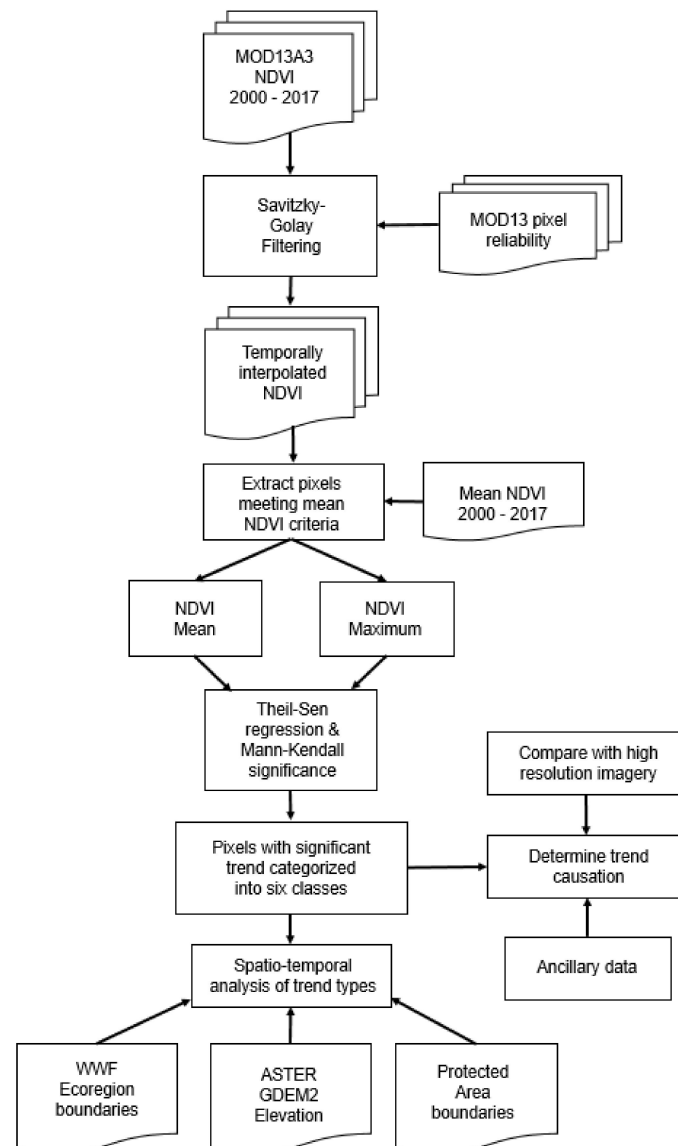
Figure 2. Workflow of the remote sensing pre-processing, trend analysis, and exploration of causality.

The study area comprised four MODIS tiles (*H9V9*, *H10V9*, *H10V10*, *H11V10*) ranging from 1 February 2000 to 31 January 2017 for a total of 203 monthly NDVI composites. To remove noise caused by atmospheric variability and clouds, we applied the Savitzky–Golay filtering procedure to the NDVI time series [31]. Because Peru is in the tropical latitudes where the growing season is year-round, we used all 12 monthly NDVI composites for all years. Our analysis was conducted on only those pixels with vegetation cover. We identified only those pixels with vegetation cover by calculating the mean NDVI of the 18 years and applied a threshold of mean annual NDVI ≥ 0.2. Any pixel with a mean annual NDVI value <0.2 was removed from the dataset prior to the trend analysis. Next, we calculated the annual maximum NDVI (NDVI-max) and annual mean NDVI (NDVI-mean) for each pixel for each of the 18 years.

2.3. MODIS Normalized Difference Vegetation Index Trend Analysis

The identification of greening and browning trends was performed using the non-parametric Thiel-Sen (TS) regression on both the NDVI-mean and the NDVI-max time-series. The TS regression was calculated for each pixel by determining the slope between every pairwise combination of NDVI composites in the time series and then finding the median value [32]. The TS median trend with a breakdown bound of 29% of the length of time-series (i.e., number of wild values that can occur within a series before it can affect the median trend) improves upon the limitations of parametric methods (e.g., OLS regression) because it is less affected by outliers, particularly in the case of small sample data (n = 18 in this study). The significance of vegetation greenness and brownness trends was evaluated using the non-parametric Mann–Kendall test [33] by considering statistical significance at the 99% confidence level ($p < 0.01$).

By combining two matrices, NDVI-mean and NDVI-max, we produced six statistically significant trend categories of change with three levels of confidence (Table 1). When a pixel had a significant trend in both NDVI-mean and NDVI-max, then it was considered to have the highest confidence of changing vegetation greenness (Both Positive and Highest Greening, Both Negative and Highest Browning). The second level of confidence was when a pixel trend was significant in only NDVI-mean (Positive Mean NDVI and Robust Greening, Negative Mean NDVI and Robust Browning). The third and lowest confidence level was when a pixel trend was significant in only NDVI-max (Positive Max NDVI and Strong Greening, Negative Max NDVI and Strong Browning).

Table 1. The six statistically significant vegetation trend categories and corresponding confidence levels. NDVI refers to the Normalized Difference Vegetation Index.

Trend Type		Confidence Level
Both Positive		Highest Greening
Positive Mean NDVI		Robust Greening
Positive Max NDVI		Strong Greening
Negative Max NDVI		Strong Browning
Negative Mean NDVI		Robust Browning
Both Negative		Highest Browning

Finally, we evaluated the trend categories for the country overall, then by PA status, biome, elevation, and by biome and elevation. The four biomes are from the World Wildlife Fund terrestrial ecoregion map [34] and biome names were adapted from Antonelli et al. [35]. There are 94 protected areas in Peru's national system and all were used in this analysis (http://geo.sernanp.gob.pe/geoserver/principal.php). The elevation source was ASTER GDEM V2 (https://gdex.cr.usgs.gov/gdex/) and the elevation range was binned into thirty 200 m elevation classes.

2.4. Exploring Causality

To investigate the potential causes of change in vegetation greenness across Peru, we compared pixels representing the highest confidence levels of change (Highest Greening and Highest Browning) with co-located higher spatial resolution data (≤30 m) on Google Earth Pro for 2000 and 2016 (2017 imagery was not available on Google Earth Pro at the time of analysis). In each of the four biomes, pixel trajectories representing Highest Greening and Highest Browning were generated through the time series. We then qualitatively compared the pixel trajectories to the observed changes in the finer grain imagery and we drew on peer-reviewed literature and field expertise for causality factors.

3. Results

3.1. Peru Overall

During the 18-year period under study, there was a general greening trend across Peru. An area of 34,398 km^2 showed a statistically significant trend of changing vegetation greenness overall, representing 3.06% of the total geographic area of Peru. Of that, 9152.70 km^2 showed browning versus 25,244.68 km^2 that showed greening (Table 2).

Table 2. Total area and relative proportion of vegetation change from 2000 to 2017 by trend type ($p < 0.01$).

| Trend Type	Area (km^2)	% of Pixels with Significant Trend
Both Positive	6448.3	18.7
Positive Mean NDVI	7257.1	21.1
Positive Max NDVI	11,539.1	33.5
Negative Max NDVI	3005.9	8.7
Negative Mean NDVI	2766.0	8.0
Both Negative	3380.7	9.8
Total	34,398	100

3.2. By Protected Area Status

The general greening signal is also evident when analyzing by PA status. In Peru, the majority of greening occurred outside the national system of PAs (Figure 3). The total area of changing vegetation outside PAs that was statistically significant was 31,880 km^2, or 92% of the statistically significant total area of vegetation change. In comparison, the area inside PAs that greened or browned was only 2520 km^2, or 7.3%. Inside PAs, 2028 km^2 greened between 2000 and 2017 whereas 492 km^2 browned. Outside PAs, 23,217 km^2 greened and 8663 km^2 browned.
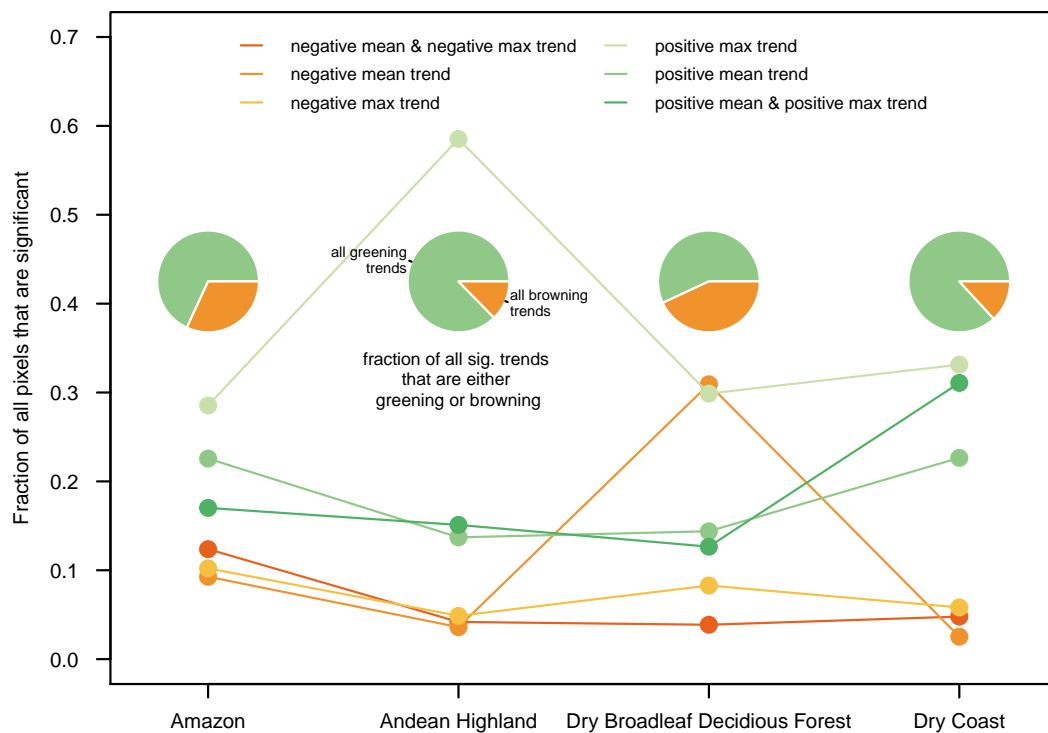
3.3. By Biome

The trends of vegetation change were different by biome, but there were greening hotspots in the Amazon, Andean Highlands, and Drylands where strong greening trends outpaced browning (Figure 4). The largest difference between greening and browning was in the Drylands biome. We calculated that 31.0% of the total area in the Drylands showed Highest Greening (both mean-NDVI and max-NDVI positive), whereas 4.8% was Highest Browning (both mean-NDVI and max-NDVI negative). In the Andean Highlands, 15.1% of the total area in the biome was categorized as Highest Greening and 4.1% was Highest Browning. The Amazon reported similar contrasts between greening and browning: 17.0% was Highest Greening and 12.4% was Highest Browning. In the TSDBF, the greening and browning signals were mixed. In the highest confidence categories, 12.6% were Highest Greening and 3.9% was Highest Browning. The largest changes were in 30.9% in Robust Browning and 29.9% in Strong Greening.
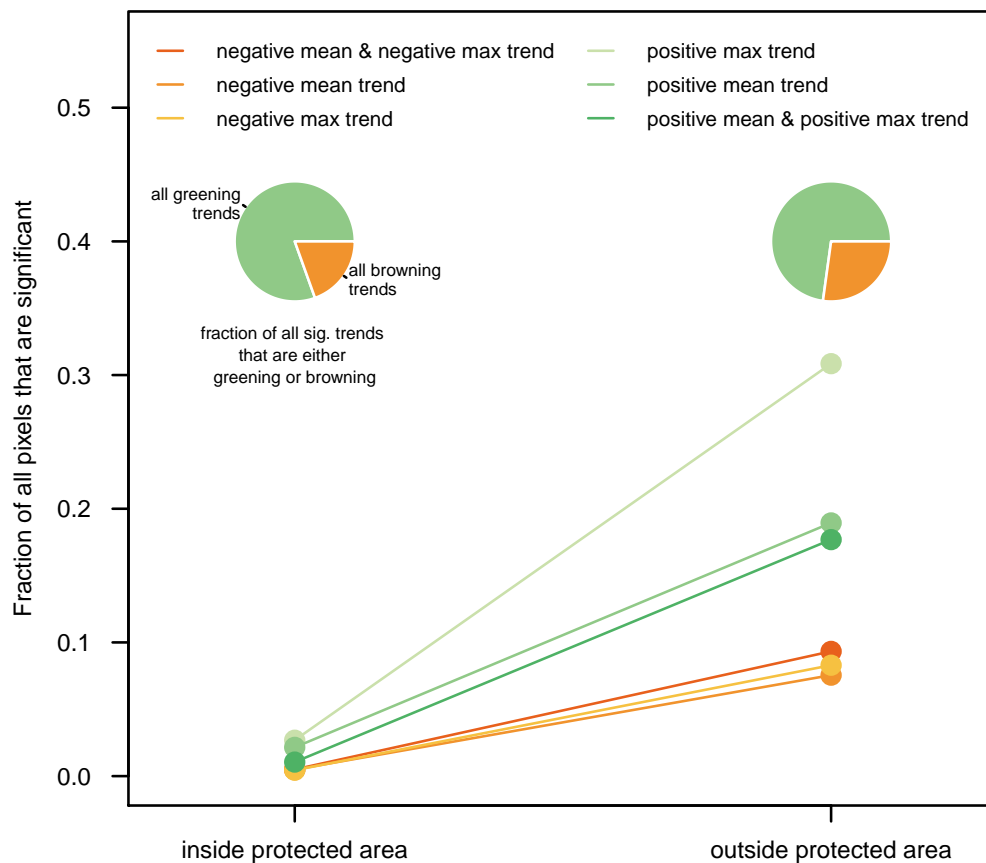
Figure 3. Greening and browning by protected area status represented as a fraction of the statistically significant area of changing vegetation for Peru. More greening occurred outside protected areas than inside.

Figure 4. Greening and browning trends by biome. Greening outpaces browning in the Amazon, Andean Highlands, and Dry Coast. Refer to Table 1 for greening and browning confidence levels.

3.4. By Elevation

Greening trends varied across the elevation gradient, switching from greening, to browning, and then back to greening as elevation increases (Figure 5). Most greening occurred between sea level and 1000 m. At elevations >1000 m and <5000 m, browning was dominant. Above 5000 m, there was more greening than browning. The highest number of significant pixels was between sea level and 1000 m, as shown in the top panel of Figure 5, corresponding with the greening signal outpacing browning. A second large cluster of pixels is between 3800 m and 5000 m, where browning is greater than greening.
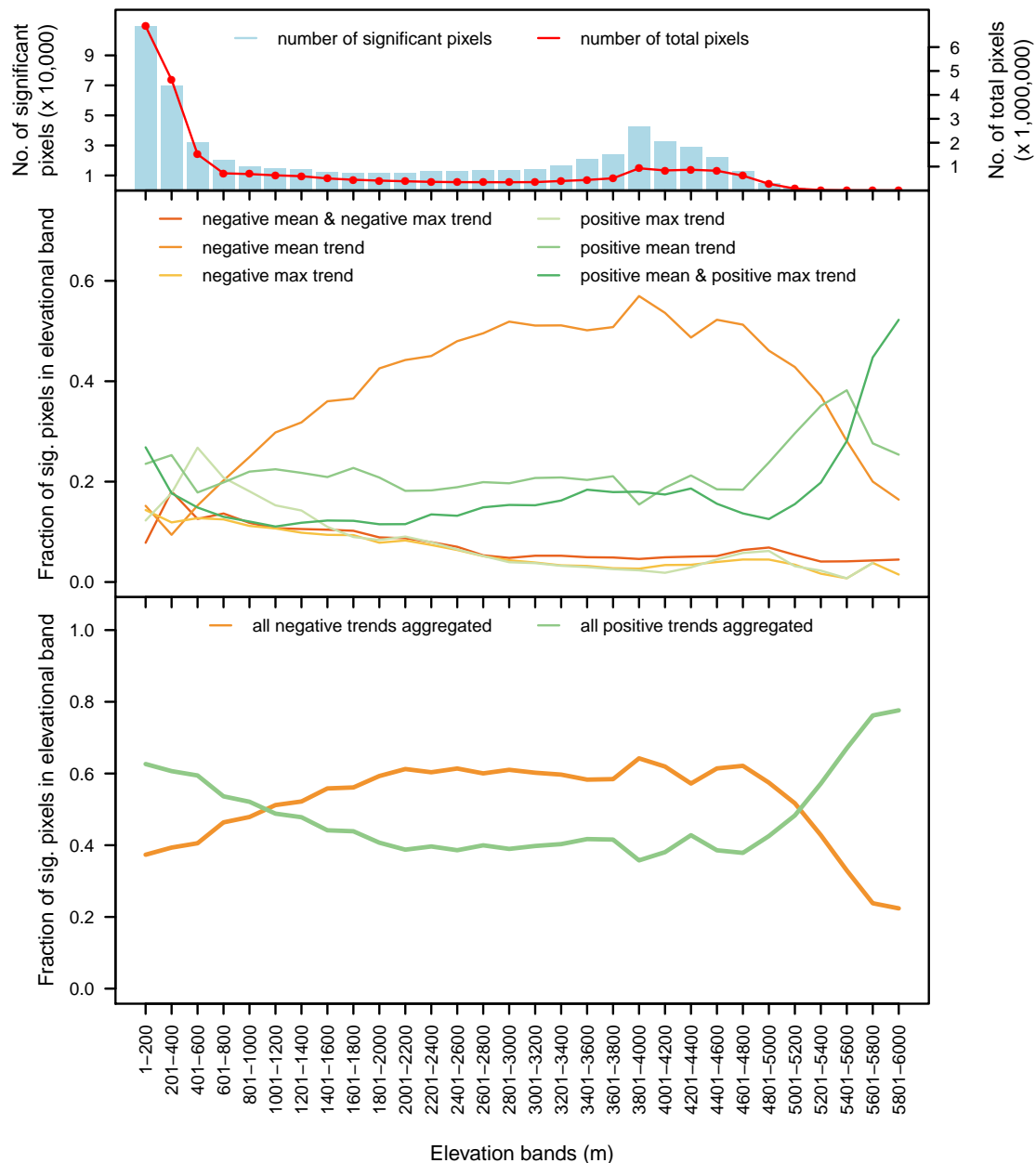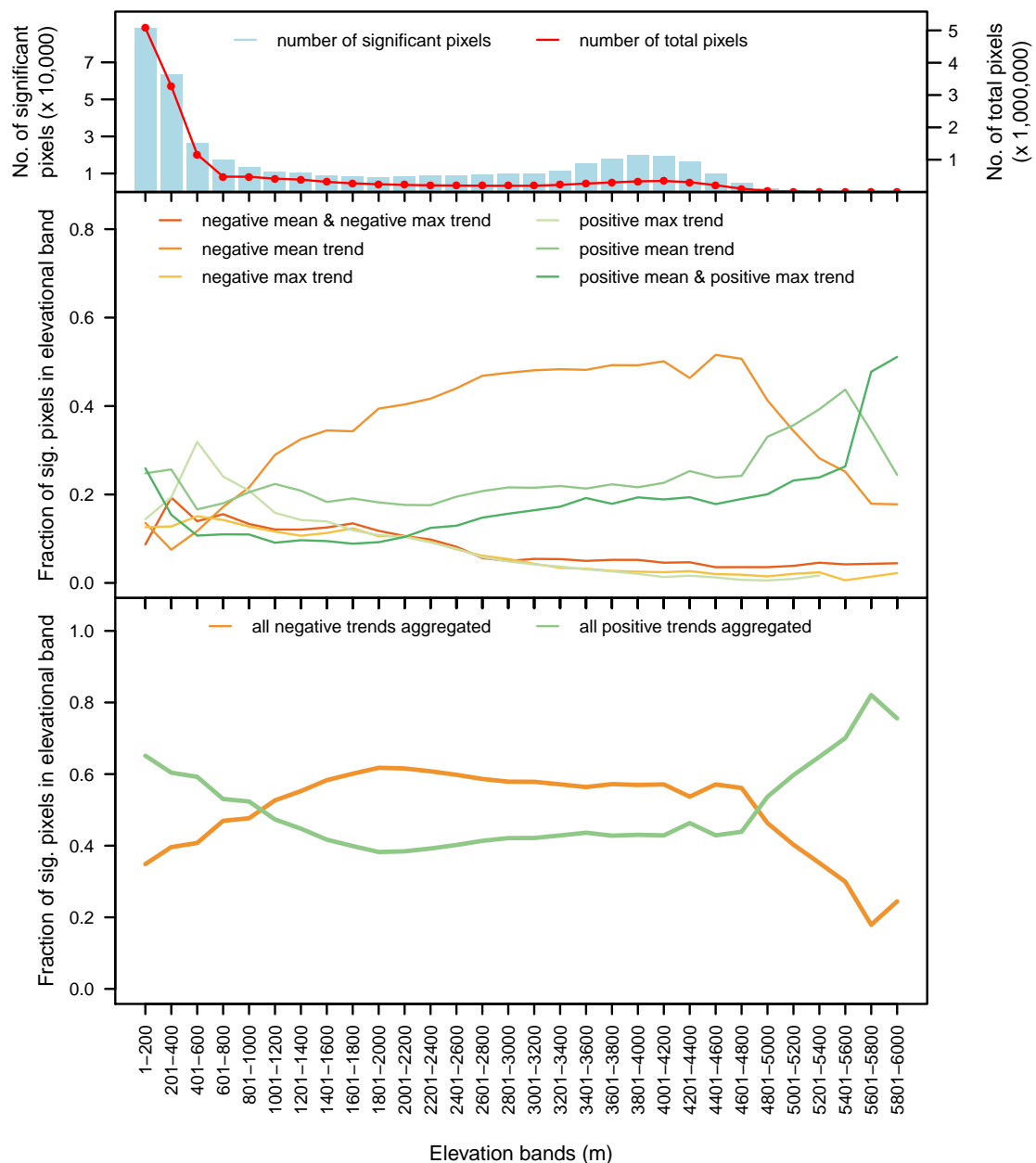

Figure 5. Greening and browning trends by elevation classes for all Peru. The top panel represents the total number of pixels (red line) and the number of statistically significant pixels (blue bars). The middle panel displays all six trend types (see Table 1 for confidence levels). The bottom panel displays all size trend types aggregated. Across the elevation gradient, greening and browning varies: greening dominated at elevations <1000 m, then switching to browning >1000 m and <5000 m, and greening at the highest elevations over 5000 m.

3.5. By Biome and Elevation

In the Amazon, the majority of greening was in the lowlands at elevations <1000 m (Figure 6). The highest reaches of the Amazon forest occur on the eastern slopes of the Andes and in these areas, browning was found at elevations from 3800 to 4600 m. The Andean Highlands as defined in Figure 1 combine both dry and humid puna (tropical alpine ecosystem types). Most of the statistically significant pixels are between 4200 and 5200 m and are browning (Figure 7). Above 5200 m, greening outpaces browning where ecological succession is occurring in post-glacial landscapes.
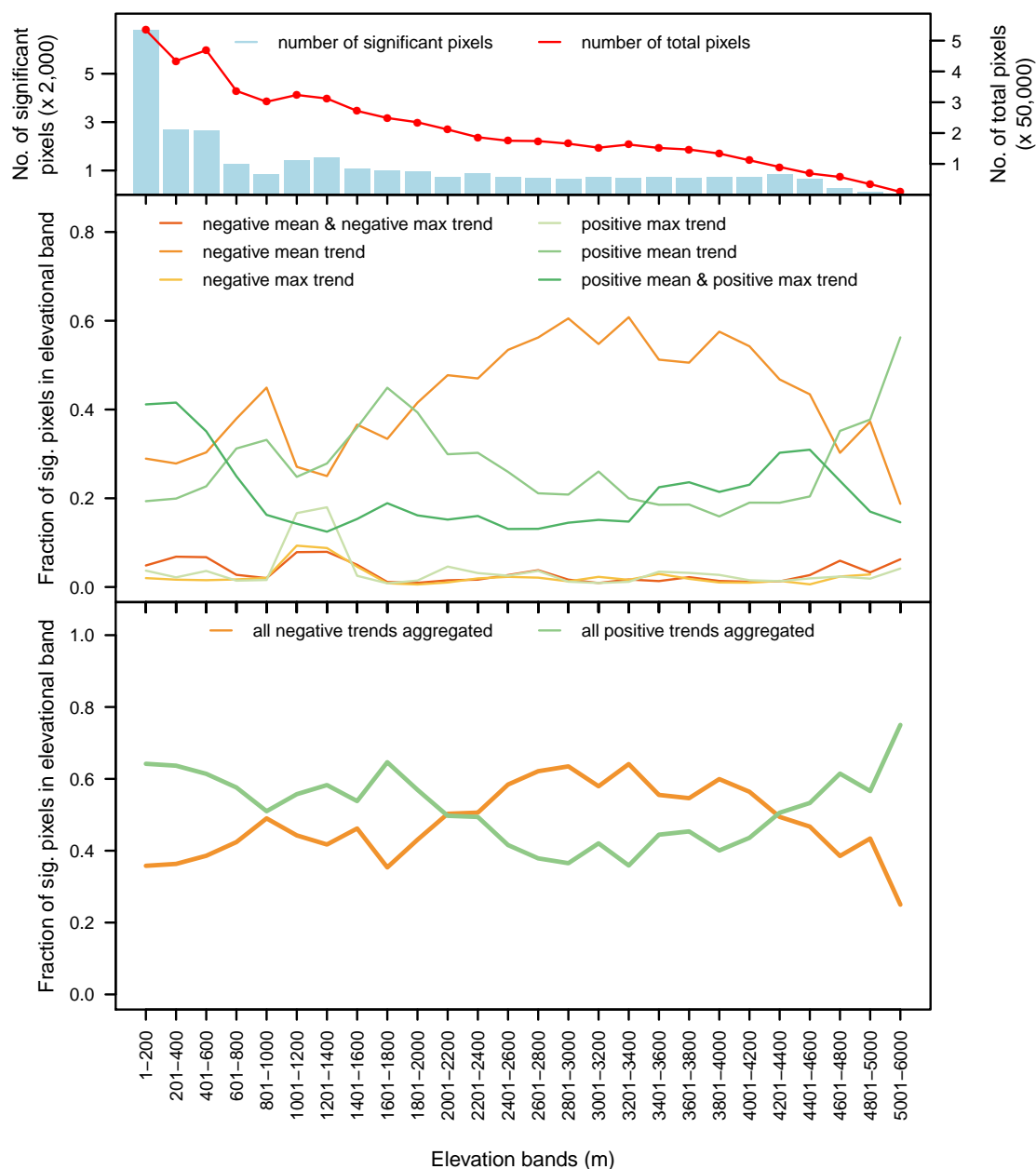

Figure 6. Greening and browning trends in the Amazon by elevation. The majority of greening, as measured by the number of significant pixels, was in the lowlands at elevations <1000 m. Refer to the caption in Figure 5 for panel descriptions.
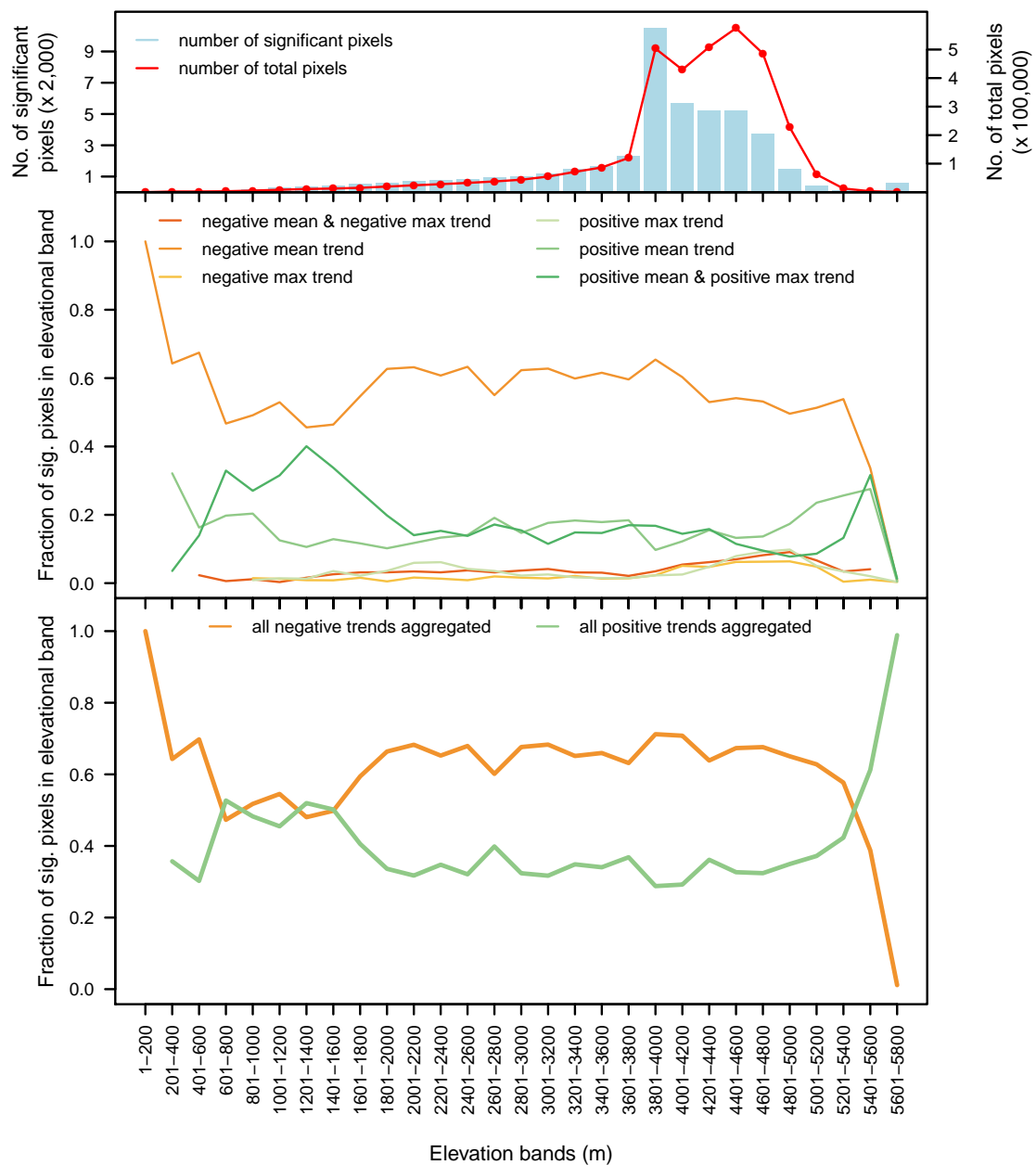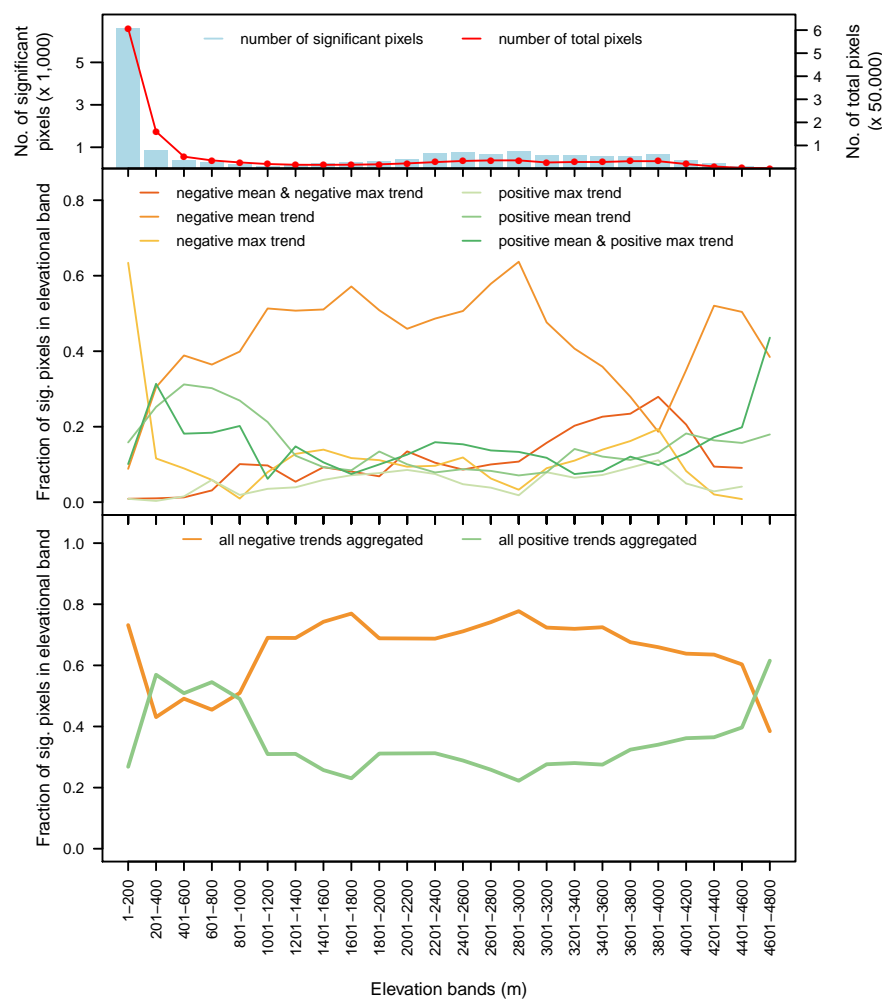
Figure 7. Greening and browning trends in the Andean Highlands by elevation. Most pixels are between 4200 and 5200 m and are browning. Above 5200 m, ecological succession in post-glacial landscapes is a greening process. Refer to the caption in Figure 5 for panel descriptions.

In the Drylands, there is a strong greening signal from sea level to 2000 m (Figure 8) related to agricultural expansion on the coastal plain. Above 2000 m and below 4200 m, browning dominates, although the number of statistically significant pixels is relatively small. Above 4000 m, greening leads browning.

Figure 8. Greening and browning trends in the Drylands by elevation. There is a strong greening signal from sea level to 2000 m, an elevation range where most significant pixels are located. Refer to the caption in Figure 5 for panel descriptions.

In the TSDBF, the vast majority of change was at elevations below 200 m (Figure 9), where browning strongly overshadows greening. There is a small area between 200 and 800 m that shows greening and, over 800 m, the trend is browning.

Figure 9. Greening and browning trends in the Tropical Subtropical Dry Broadleaf Forest (TSDBF) by elevation. The vast majority of change was <200 m, where browning overshadows greening. Refer to the caption in Figure 5 for panel descriptions.

4. Discussion

Over an 18-year period across Peru, greening trends outpaced browning. The vast majority of Peru's vegetation (97%) showed no change in greenness over the study period, similar to stable trends evaluated in China from 2000 to 2010 [36]. By protected area status, we found that the majority, or 92%, of greening occurred outside PAs. Further analysis by biome and elevation showed that greening and browning trends were variable. By Peru's four major biomes, we found that greening was dominant in the Andean Highlands, Amazon and in the Drylands, whereas the signal was mixed in the TSDBF. Across the elevation gradient, greening outpaced browning at the lower and higher elevation classes, but browning overrode greening in the mid-elevation classes. When evaluated by biome and elevation, the trends were variable and imply that different drivers must be at work.

4.1. Drivers of Greening and Browning Inside Protected Areas

Given active management and restoration efforts inside PAs, we expected that greening would be related to conservation status. That is, greening would be more likely to occur inside Peru's national system of PAs and browning would be higher outside PAs where human disturbance is more prevalent. In China, greening has been associated with PA status, although greening trends vary depending on the PA category [36]. In and around Colombia's Picachos National Park there was net greening within in the park and net browning outside the park, but both were temporally variable [37]. At the scale of

Europe, Buitenwerf et al. [38] used MODIS LAI to compare greening and browning inside vs. outside PAs; they found no difference and concluded that conservation efforts are not a factor in greening. Our findings are in contrast with examples from China, Colombia, and Europe because there is more greening outside PAs than inside. We believe that the drivers of greening outside PAs would likely be anthropogenic. If PAs determined that greening is a desired process, land management practices could be designed and implemented for such goals and where they are ecologically and socially appropriate. The PAs may serve as a type of experimental control, in that they show that global forcers are less of a factor in explaining Peru's dynamism than human land use. Peru has ten national PA categories plus private conservation areas and regional conservation areas; future work could explore the effect of the category on greening/browning in order to examine in more detail links between land management policies and changes in vegetation cover.

4.2. Drivers of Greening and Browning by Biome and Elevation

We expected that there would be similar NDVI patterns in the four major biomes, but instead found that each biome's NDVI trends are different, especially when elevation gradients are taken into account. These differences are likely due to processes and drivers of change specific to each biome and elevation range. To explore the potential causalities of both greening and browning within biomes and by elevation, we compared high-resolution imagery from 2000 to 2016 (2017 was not available at the time of analysis) with a single pixel NDVI value through the same 17-year trajectory. This was performed for greening and browning at representative sites in the four biomes that were selected by our extensive knowledge and field experience in each of the biomes (Figures 10–15).
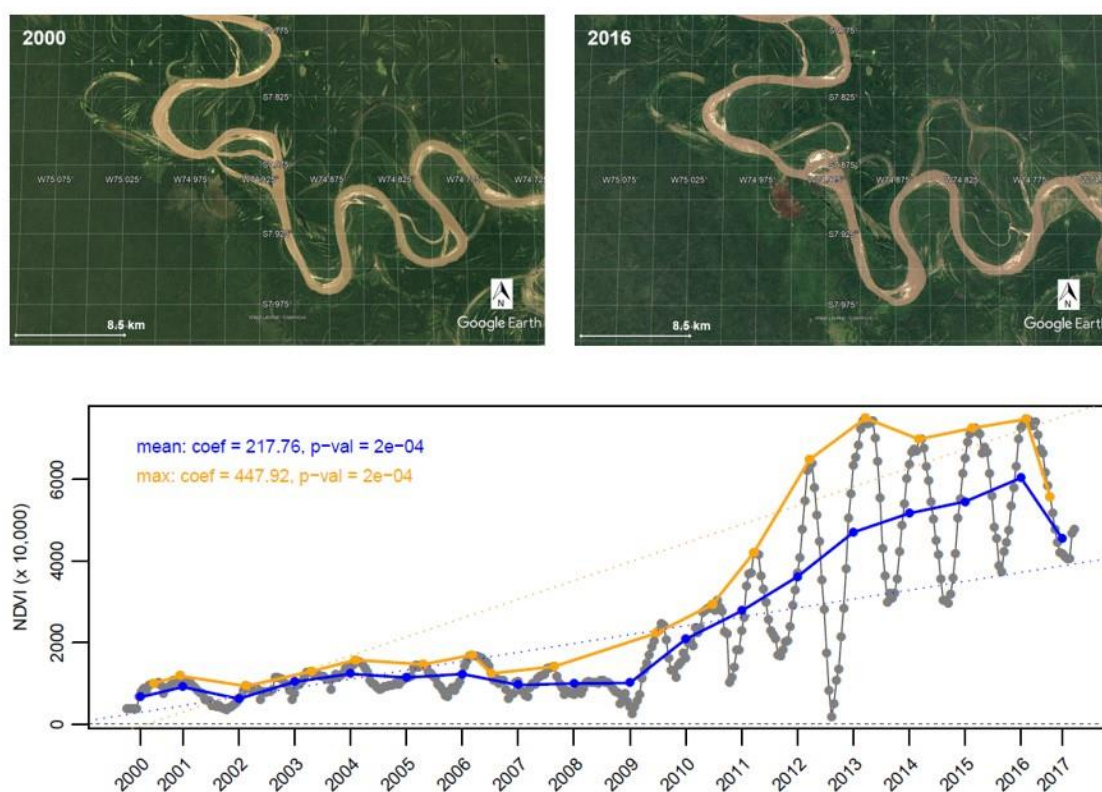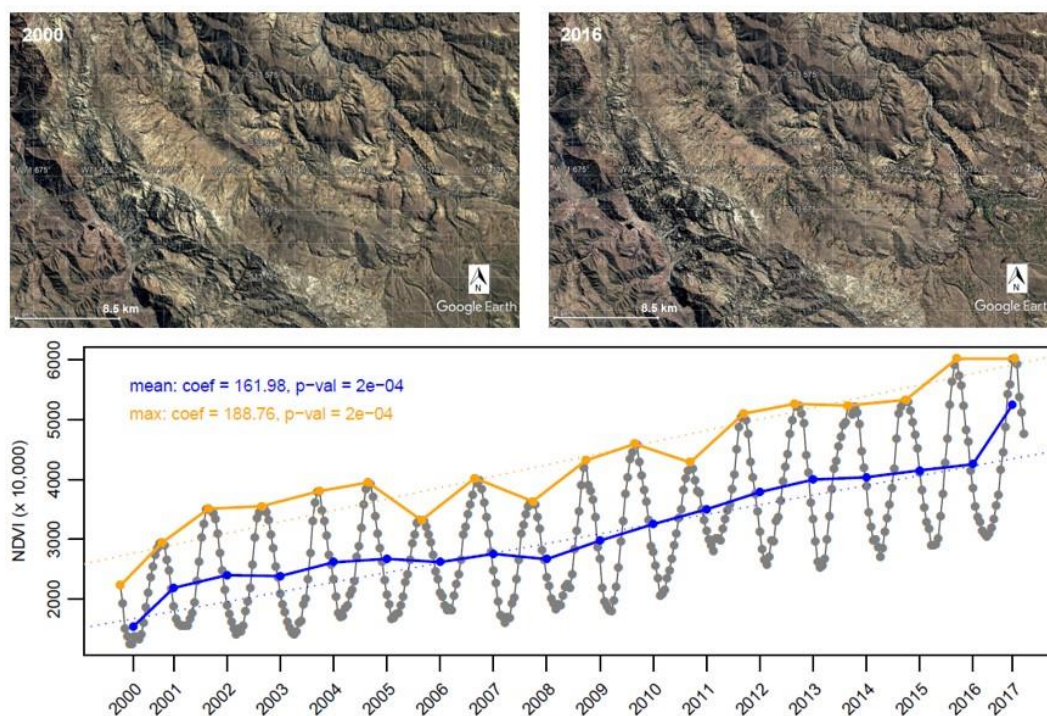

Figure 10. In the upper panels, high spatial resolution imagery from Google Earth Pro shows Amazon greening downriver from Pucallpa between 2000 and 2016. Deposition of sediment creates substrates on which forest succession can occur and appears as a positive NDVI trend. The accompanying graph shows the entire time-series of the NDVI data and fitted Thiel-Sen trends for NDVI-mean (blue) and NDVI-maximum (orange) for a pixel located at S 7.874447°, W 74.916197°.
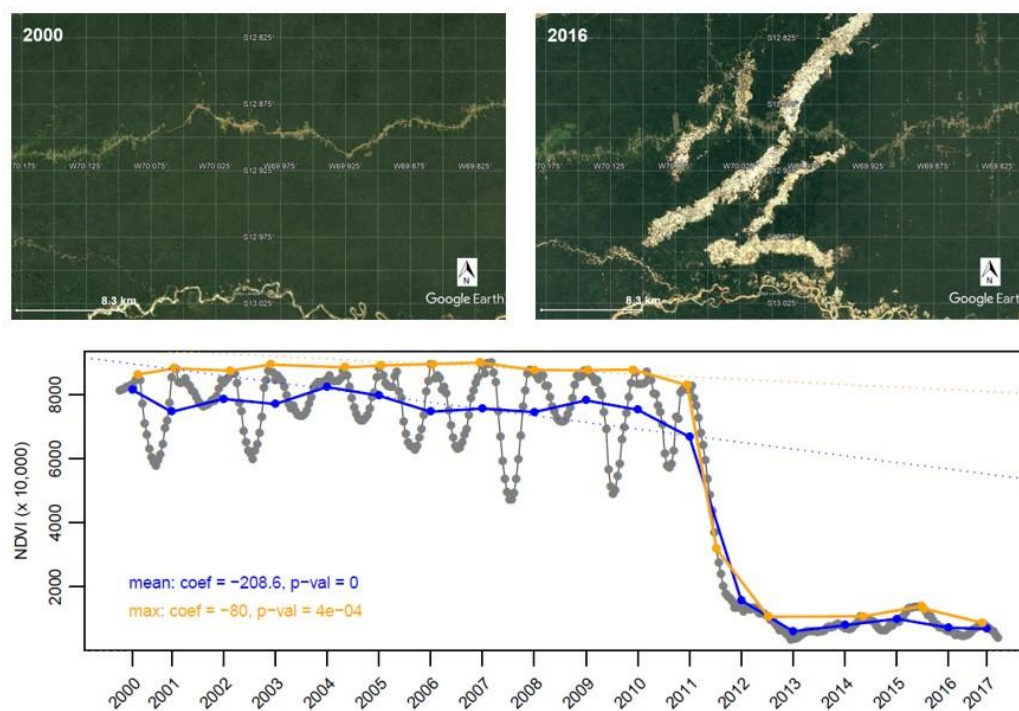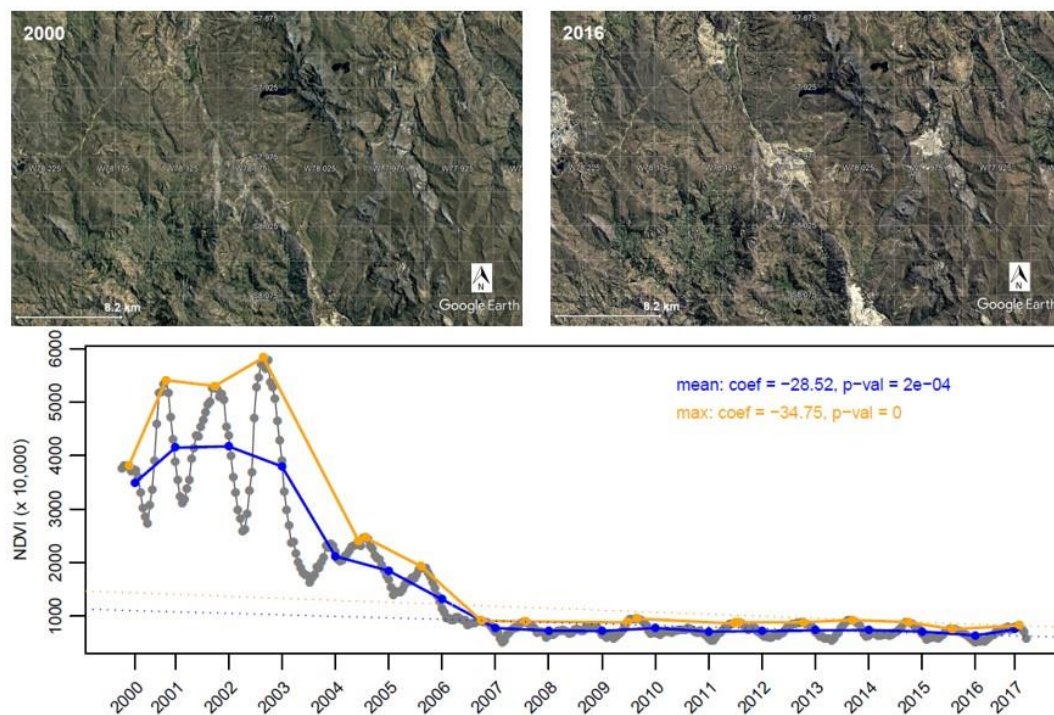
Figure 11. In the upper panels, high spatial resolution imagery from Google Earth Pro shows Amazon browning near Madre de Dios between 2000 and 2016. Removal of vegetation for mining results in a distinct stair-step NDVI trend. The accompanying graph shows the entire time-series of the NDVI data and fitted Thiel-Sen trends for NDVI-mean (blue) and NDVI-maximum (orange) for a pixel located at S 12.921817°, W 70.007838°.
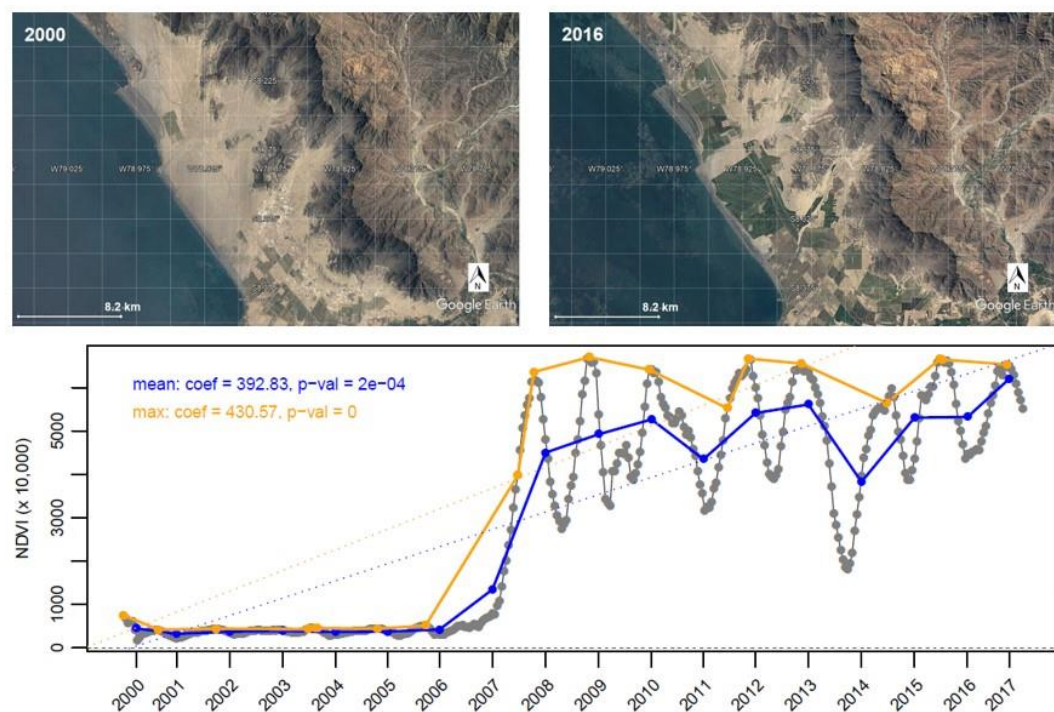

Figure 12. In the upper panels, high spatial resolution imagery from Google Earth Pro shows Andean Highlands greening east of Cusco between 2000 and 2016. Expanding pine and eucalyptus plantations are likely drivers of gradual greening in this region. The accompanying graph shows the entire time-series of the NDVI data and fitted Thiel-Sen trends for NDVI-mean (blue) and NDVI-maximum (orange) for a pixel located at S 13.662586°, W 71.522592°.
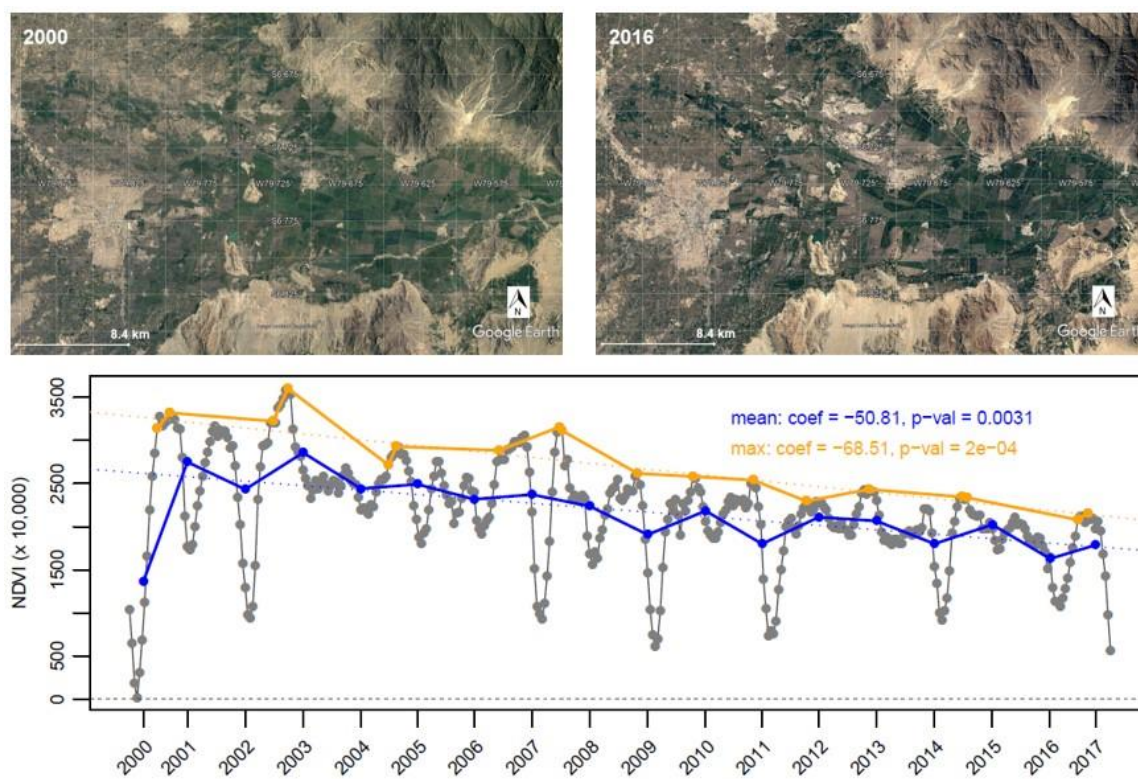
Figure 13. In the upper panels, high spatial resolution imagery from Google Earth Pro shows browning in the Andean Highlands near La Libertad between 2000 and 2016. Expanding mine footprints result in rapid decreases in NDVI. The accompanying graph shows the entire time-series of the NDVI data and fitted Thiel-Sen trends for NDVI-mean (blue) and NDVI-maximum (orange) for a pixel located at S 7.977320°, W 78.086017°.

Figure 14. In the upper panels, high spatial resolution imagery from Google Earth Pro shows Dry Coast greening south of Trujillo between 2000 and 2016. Agricultural land use is expanding on the Dry Coast and converts desert to agriculture that produces greening signals in the data. The accompanying graph shows the entire time-series of the NDVI data and fitted Thiel-Sen trends for NDVI-mean (blue) and NDVI-maximum (orange) for a pixel located at S 8.312944°, W 78.914959°.

Figure 15. In the upper panels, high spatial resolution imagery from Google Earth Pro shows Dry Coast browning near Lambayeque between 2000 and 2016. Where urban centers expand into agricultural zones, a loss of vascular plant material results in browning trends. The accompanying graph shows the entire time-series of the NDVI data and fitted Thiel-Sen trends for NDVI-mean (blue) and NDVI-maximum (orange) for a pixel located at S 6.762088°, W 79.727939°.

In the Amazon, greening is likely affected by two different drivers. Our research revealed distinct patterns of greening and browning around rivers indicating that the lateral migration of river channels plays an important role in causing ecological change (Figure 10). Deposition of sediment creates substrates on which forest succession can occur. Erosion removes substrates and vegetation, but our data show that the deposition-forest succession process is more spatially dominant. Outside fluvial settings, greening could be the result of forest regrowth following abandonment. Declines in agricultural productivity due to soil fertility losses often lead to abandonment and allow for forest recovery. Post-agricultural tropical forest recovery varies depending on land use features, related disturbance characteristics, and the state of the matrix [39], but could appear as greening. Browning in the Amazon is connected to the effects of mining when vegetation is removed to facilitate extraction. The Madre de Dios region is emblematic of this deforestation and fragmentation process and the trend line is a stair-step representing a rapid transition from a vegetated state to a de-vegetated state (Figure 11).

The greening we document in the Peruvian Andean Highlands corroborates previously published research. Vegetation dynamism is characteristic of Andean treelines and in post-glacial landscapes [40,41]. After glaciers retreat, new substrates are revealed and primary succession can occur. Pine and eucalyptus plantations are expanding to meet increasing timber demand from mining operations and urban growth, greening that is identifiable on high spatialresolution images (Figure 12). Treelines are expanding upslope as tree seedlings and woody plants encroach into neighboring grasslands [14,42–44]. Another greening effect is the expansion of high-altitude wetlands (*bofedales*) in some sites as shown by increasing NDVI [45]. The geographic boundary of Andean Highlands we used includes both humid and dry puna, which are two distinct ecosystems in northern and southern Peru. A possible driver of browning in the Andean Highlands could be shrubby elements of the

dry puna expanding into the humid puna. On the other hand, shrublands are increasing into high elevation zones, a process that could result in greening [15]. Emigration from remote mountain areas to urban centers can lead to abandonment of farming plots that then convert to shrublands or forests [46]. Rural-to-urban migration can be also linked to browning because urban zones expand to accommodate immigration. Mining is another driver of browning in the highlands. High metal commodity prices put pressure on extractive activities that result in expanded mine footprints and large drops in NDVI (Figure 13).

In the arid and hyper-arid Drylands, greening outpaced browning in low and high elevations. One likely driver of greening along the coastal plain is the expansion of agriculture meant for exports. For example, the Chavimochic and Chinecas irrigation projects south of Trujillo divert glacier meltwater from the Santa river basin to large agricultural areas that have steadily grown in extent over the last 50 years [47,48]. The sudden increase in NDVI values shown in Figure 14 illustrate the expansion of this kind of agriculture. The Majes Siguas Special Project in southern Peru exhibits the same NDVI trajectories. Note that browning in the Drylands at low elevations might also be related to the transition of crop types over time. In some cases, the extent of cropland does not change, but the NDVI trend is negative, so we surmised that crop types within the zones may change due to decreasing water availability, soil degradation, and changes in consumer preferences (increasing demand for blueberries and asparagus, for example). Coastal browning is also observed where urban centers expand into agricultural zones resulting in a loss of vascular plant material (Figure 15). The expansion of urban areas and mines would account for browning in mid to high elevations as well. At the highest elevation in the Drylands biome, the processes would be similar to the Andean Highlands, related to increases in shrublands and ecological succession after glacier retreat.

Other contributions to greening in Peru are the potential interactions with El Niño events. Undisturbed areas of Drylands are mostly devoid of vegetation except for fog-dependent plant communities, or *lomas*. Following El Niño events, *lomas* respond to the increase in precipitation by increasing abundance, changing species composition, and increasing cover and extent. These are responses that should be apparent in NDVI values, although van Leeuwen et al. [49] note that an anomaly in NDVI time series data could influence the relationship between NDVI and El Niño, at least as derived from AVHRR. Biocrusts and *lomas* are admixed and this combined with low vegetation cover presents remote sensing challenges, but recent work offers potential solutions. Panigada et al. [50] reported using high temporal, spatial, and spectral data from Sentinel-2 to monitor dryland biocrusts in the Negev Desert along a precipitation gradient. This type of approach could be applied in Peru's biomes with El Niño indices used and MODIS data to parse out the relationship between NDVI and cyclical rainfall.

In the TSDBF biome, the greening and browning signals are less clear as multiple ecosystem types exist in a smaller area. The El Niño signal impacts TSDBF on western and northern slopes and this is the part of Peru most altered by ENSO-related changes. But the pervasiveness of middle elevation browning instead suggests that the deforestation front reported for that area supplies much of the change [15]. The NDVI trends for deciduous trees in South America reported by Fensholt et al. [51], were positive from 1982–2011, which would fit with lower elevation greening where tropical dry forests can be found, but would also include the new agricultural areas in lowland north Peru.

4.3. Caveats and Additional Considerations

This study fitted a linear model to characterize statistically significant changes in an NDVI time-series. We recognize, however, that drivers of change and vegetation responses can be non-linear. For example, mining in the Andes and Amazon produces a stair-step change from a vegetated to non-vegetated state. Coastal landscapes green following El Niño-induced precipitation events that are pulses over a 3 to 7-year cycle; TSDBF is also affected by El Niño events. Deforestation for agricultural land use, subsequent abandonment, and recovery could produce a U-shaped NDVI trend line that a linear model might report as a slow decrease or increase. By using NDVI-max and NDVI-mean in

the trend analysis, our approach also removed the influence of seasonality that influences vegetation greenness annually. In the past decade, several different time-series analysis methods have been developed that are able to explicitly include and model seasonality [52], as well as both gradual and abrupt changes in vegetation greenness over time [53]. Our future research will focus on testing these improved modeling techniques on the MODIS NDVI time-series data. Also, given the high spatial heterogeneity and fine scale diversity in vegetation types and land use in Peru, 1 km pixel resolution is not optimal. Higher spatial resolution time-series would enable more accurate representation of spatial vegetation greenness patterns and their drivers, which would be directly relevant to land-management interventions. Besides spatial resolution, a longer time-series of vegetation indices is also desirable since inter-annual vegetation dynamics are impacted by longer climatic cycles.

Lagged effects have also been noted for Andean vegetation and precipitation [54] and primary succession lags after glacier recession [55]. Future work on similar questions could employ non-linear techniques such as the Breaks For Additive Seasonal and Trend (BFAST) method that decomposes the observed trends into linear multi-year trends and seasonality in which non-trivial and significant jumps and breaks reflecting important ecological events or shifts are detected; this would allow for disentangling vegetation responses at a finer temporal resolution [53]. Future work can also include more formal models of causality that go beyond correlation and lagged regression and provide a robust estimate of true causation where multiple variables and multiple lags are tested simultaneously thus avoiding spurious and indirect causation [56,57]. Furthermore, we are aware of the literature documenting uncertainties and challenges of measuring greening in the Amazon using MODIS data as well as the complexities and sensitivities of Amazon vegetation dynamics to rainfall, seasonality, drought, and atmospheric conditions, among others, and future work would account for these variables.

5. Conclusions

The Earth is greening [16] and our results show that landscape change in Peru fits within global trends. Peru is greening overall, but with its high biological, ecological, and topographic diversity, general greening trends mask finer-scale changes. Using the finest level of detail (smallest pixel size) available with the longest temporal extent, we combine that with co-located higher spatial resolution data to explore likely drivers of change that differ from biome to biome, across elevations, and by protected area status. Our explorations of drivers of greening and browning are probable, but merit additional research. They serve as hypotheses for future research that would expand on the Earth science fundamentals elucidated by Alexander von Humboldt, but acknowledging that his attention to the human dimensions of change is all the more relevant for understanding land-cover changes. As a result, we conclude by confirming the opportunities described by Schrodt et al. [9] to celebrate Humboldt's contributions by using new technologies but applying them to describe processes driven by global economic and biophysical changes, but as mediated through landscape-level processes acting through human–environment dynamics.

the academic and logistical home in Lima provided for many years by San Marcos University's Natural History Museum (Museo de Historia Natural, UNMSM).

References

1.   Von Humboldt, A. *Views of the Cordilleras and Monuments of the Indigenous Peoples of the Americas*; University of Chicago Press: Chicago, IL, USA, 2012.

2.   Von Humboldt, A. *Political Essay on the Kingdom of New Spain*; Volume 1, University of Chicago Press: Chicago, Il, USA, 2019.

3.   Von Humboldt, A. *Political Essay on the Kingdom of New Spain*; Volume 2, University of Chicago Press: Chicago, Il, USA, 2019.

4.   Von Humboldt, A.; Bonpland, A. *Essay on the Geography of Plants*; Jackson, S.T., Romanowski, S., Eds.; Reprint; University of Chicago Press: Chicago, IL, USA, 2009.

5.   Lack, H.W. *Alexander von Humboldt: The Botanical Exploration of the Americas*; Prestel: Munich, Germany, 2018.

6.   Zimmerer, K.S. Humboldt's nodes and modes of interdisciplinary environmental science in the Andean world. *Geogr. Rev.* **2006**, *96*, 335–360. [CrossRef]

7.   Morueta-Holme, N.; Engemann, K.; Sandoval-Acuña, P.; Jonas, J.D.; Segnitz, R.M.; Svenning, J.-C. Strong upslope shifts in Chimborazo's vegetation over two centuries since Humboldt. *Proc. Natl. Acad. Sci. USA* **2015**, *112*, 12741–12745. [CrossRef] [PubMed]

8.   Moret, P.; Muriel, P.; Jaramillo, R.; Dangles, O. Humboldt's Tableau Physique revisited. *Proc. Natl. Acad. Sci. USA* **2019**, *116*, 12889–12894. [CrossRef] [PubMed]

9.   Schrodt, F.; Santos, M.J.; Bailey, J.J.; Field, R. Challenges and opportunities for biogeography—What can we still learn from von Humboldt? *J. Biogeogr.* **2019**, *46*, 1–12. [CrossRef]

10. Millington, A.; Jepson, W. (Eds.) *Land Change Science in the Tropics: Changing Agricultural Landscapes*; Springer: New York, NY, USA, 2008.

11. Boillat, S.; Scarpa, F.M.; Robson, J.P.; Gasparri, I.; Aide, T.M.; Aguiar, A.P.D.; Anderson, L.O.; Batistella, M.; Fonseca, M.G.; Futemma, C.; et al. Land system science in Latin America: Challenges and perspectives. *Curr. Opin. Environ. Sustain.* **2017**, *26–27*, 37–46. [CrossRef]

12. Rodríguez, L.O.; Young, K.R. Biological diversity of Peru: Determining priority areas for conservation. *AMBIO* **2000**, *29*, 329–337. [CrossRef]

13. Young, K.R.; Rodríguez, L.O. Development of Peru's national protected area system: Historical continuity in conservation goals. In *Globalization and New Geographies of Conservation*; Zimmerer, K.S., Ed.; University of Chicago Press: Chicago, IL, USA, 2006; pp. 229–254.

14. Aide, T.M.; Clark, M.L.; Grau, H.R.; López-Carr, D.; Levy, M.A.; Redo, D.; Bonilla-Moheno, M.; Riner, G.; Andrade-Núñez, M.J.; Muñiz, M. Deforestation and reforestation of Latin America and the Caribbean (2001–2010). *Biotropica* **2013**, *45*, 262–271. [CrossRef]

15. Aide, T.M.; Grau, H.R.; Graesser, J.; Andrade-Nuñez, M.J.; Aráoz, E.; Barros, A.P.; Campos-Cerqueira, M.; Chacon-Moreno, E.; Cuesta, F.; Espinoza, R.; et al. Woody vegetation dynamics in the tropical and subtropical Andes from 2001 to 2014: Satellite image interpretation and expert validation. *Glob. Change Biol.* **2019**, *25*, 2112–2126. [CrossRef]

16. Zhu, Z.; Piao, S.; Myneni, R.B.; Huang, M.; Zeng, Z.; Canadell, J.G.; Ciais, P.; Sitch, S.; Friedlingstein, P.; Arneth, A.; et al. Greening of the Earth and its drivers. *Nat. Clim. Chang.* **2016**, *6*, 791–795. [CrossRef]

17. Chen, C.; Park, T.; Wang, X.; Piao, S.; Xu, B.; Chaturvedi, R.K.; Fuchs, R.; Brovkin, V.; Ciais, P.; Fensholt, R.; et al. China and India lead in greening of the world through land-use management. *Nat. Sustain.* **2019**, *2*, 122. [CrossRef]

18. Parent, M.B.; Verbyla, D. The browning of Alaska's boreal forest. *Remote Sens.* **2010**, *2*, 2729–2747. [CrossRef]

19. De Jong, R.; Verbesselt, J.; Schaepman, M.E.; de Bruin, S. Trend changes in global greening and browning: Contribution of short-term trends to longer-term change. *Glob. Chang. Biol.* **2012**, *18*, 642–655. [CrossRef]

20. Mishra, N.B.; Mainali, K.P. Greening and browning of the Himalaya: Spatial patterns and the role of climatic change and human drivers. *Sci. Total Environ.* **2017**, *587*, 326–339. [CrossRef] [PubMed]

21. Houston, J.; Hartley, A.J. The central Andean west-slope rainshadow and its potential contribution to the origin of hyper-aridity in the Atacama Desert. *Int. J. Climatol.* **2003**, *23*, 1453–1464. [CrossRef]

22. Garreaud, R.D. The Andes climate and weather. *Adv. Geosci.* **2009**, *22*, 3–11. [CrossRef]

23. Young, K.R.; Leon, B.L.; Jorgensen, P.M.; Ulloa Ulloa, C. Tropical and subtropical landscapes of the Andes. In *The Physical Geography of South America*; Veblen, T.T., Young, K.R., Orme, A.R., Eds.; Oxford University Press: Oxford, UK, 2007; pp. 200–216.

24. SERNANP Listado de Áreas Naturales Protegidas. Available online: http://www.sernanp.gob.pe/el-sinanpe (accessed on 16 July 2019).

25. Kier, G.; Mutke, J.; Dinerstein, E.; Ricketts, T.H.; Küper, W.; Kreft, H.; Barthlott, W. Global patterns of plant diversity and floristic knowledge. *J. Biogeogr.* **2005**, *32*, 1107–1116. [CrossRef]

26. Joppa, L.N.; Roberts, D.L.; Myers, N.; Pimm, S.L. Biodiversity hotspots house most undiscovered plant species. *Proc. Natl. Acad. Sci. USA* **2011**, *108*, 13171–13176. [CrossRef]

27. Miraldo, A.; Li, S.; Borregaard, M.K.; Flórez-Rodríguez, A.; Gopalakrishnan, S.; Rizvanovic, M.; Wang, Z.; Rahbek, C.; Marske, K.A.; Nogués-Bravo, D. An Anthropocene map of genetic diversity. *Science* **2016**, *353*, 1532–1535. [CrossRef]

28. Rau, P.; Bourrel, L.; Labat, D.; Melo, P.; Dewitte, B.; Frappart, F.; Lavado, W.; Felipe, O. Regionalization of rainfall over the Peruvian Pacific slope and coast. *Int. J. Climatol.* **2017**, *37*, 143–158. [CrossRef]

29. Espinoza, J.C.; Chavez, S.; Ronchail, J.; Junquas, C.; Takahashi, K.; Lavado, W. Rainfall hotspots over the southern tropical Andes: Spatial distribution, rainfall intensity, and relations with large-scale atmospheric circulation. *Water Resour. Res.* **2015**, *51*, 3459–3475. [CrossRef]

30. Didan, K.; Barreto Munoz, A.; Solano, R.; Huete, A. *MODIS Vegetation Index User's Guide*; Version 3.00; Vegetation Index and Phenology Lab, The University of Arizona: Tucson, AR, USA, 2015.

31. Savitzky, A.; Golay, M.J.E. Smoothing and differentiation of data by simplified least squares procedures. *Anal. Chem.* **1964**, *36*, 1627–1639. [CrossRef]

32. Sen, P.K. Estimates of the regression coefficient based on Kendall's tau. *J. Am. Stat. Assoc.* **1968**, *63*, 1379–1389. [CrossRef]

33. Mann, H.B. Nonparametric tests against trend. *Econom. J. Econom. Soc.* **1945**, 245–259. [CrossRef]

34. Olson, D.M.; Dinerstein, E.; Wikramanayake, E.D.; Burgess, N.D.; Powell, G.V.; Underwood, E.C.; D'Amico, J.A.; Itoua, I.; Strand, H.E.; Morrison, J.C. Terrestrial ecoregions of the world: A new map of life on Earth. *BioScience* **2001**, *51*, 933–938. [CrossRef]

35. Antonelli, A.; Zizka, A.; Carvalho, F.A.; Scharn, R.; Bacon, C.D.; Silvestro, D.; Condamine, F.L. Amazonia is the primary source of Neotropical biodiversity. *Proc. Natl. Acad. Sci. USA* **2018**, *115*, 6034–6039. [CrossRef] [PubMed]

36. Lü, Y.; Zhang, L.; Feng, X.; Zeng, Y.; Fu, B.; Yao, X.; Li, J.; Wu, B. Recent ecological transitions in China: Greening, browning, and influential factors. *Sci. Rep.* **2015**, *5*, 8732. [CrossRef]

37. Murillo-Sandoval, P.J.; Van Den Hoek, J.; Hilker, T. Leveraging multi-sensor time series datasets to map short- and long-term tropical forest disturbances in the Colombian Andes. *Remote Sens.* **2017**, *9*, 179. [CrossRef]

38. Buitenwerf, R.; Sandel, B.; Normand, S.; Mimet, A.; Svenning, J.-C. Land surface greening suggests vigorous woody regrowth throughout European semi-natural vegetation. *Glob. Chang. Biol.* **2018**, *24*, 5789–5801. [CrossRef]

39. Chazdon, R.L. *Second Growth: The Promise of Tropical Forest Regeneration in an Age of Deforestation*; University of Chicago Press: Chicago, IL, USA, 2014.

40. Young, K.R. Ecology of land cover change in glaciated tropical mountains. *Rev. Peru. Biol.* **2014**, *21*, 259–270.

41. Young, K.R.; Ponette-González, A.G.; Polk, M.H.; Lipton, J.K. Snowlines and treelines in the tropical Andes. *Ann. Am. Assoc. Geogr.* **2017**, *107*, 429–440. [CrossRef]

42. Kintz, D.B.; Young, K.R.; Crews-Meyer, K.A. Implications of land use/land cover change in the buffer zone of a national park in the tropical Andes. *Environ. Manag.* **2006**, *38*, 238–252. [CrossRef] [PubMed]

43. Lipton, J.K. Human Dimensions of Conservation, Land Use, and Climate Change in Huascaran National Park, Peru. Ph.D. Thesis, University of Texas at Austin, Austin, TX, USA, 2008.

44. Rehm, E.M.; Feeley, K.J. Forest patches and the upward migration of timberline in the southern Peruvian Andes. *For. Ecol. Manag.* **2013**, *305*, 204–211. [CrossRef]

45. Mazzarino, M.; Finn, J.T. An NDVI analysis of vegetation trends in an Andean watershed. *Wetlands Ecol. Manag.* **2016**, *24*, 623–640. [CrossRef]

46. Radel, C.; Jokisch, B.D.; Schmook, B.; Carte, L.; Aguilar-Støen, M.; Hermans, K.; Zimmerer, K.; Aldrich, S. Migration as a feature of land system transitions. *Curr. Opin. Environ. Sustain.* **2019**, *38*, 103–110. [CrossRef]

47. Bury, J.; Mark, B.G.; Carey, M.; Young, K.R.; McKenzie, J.; Baraer, M.; French, A.; Polk, M.H. New geographies of water and climate change in Peru: Coupled natural and social transformations in the Santa River watershed. *Ann. Assoc. Am. Geogr.* **2013**, *103*, 363–374. [CrossRef]

48. Carey, M.; Baraer, M.; Mark, B.G.; French, A.; Bury, J.; Young, K.R.; McKenzie, J.M. Toward hydro-social modeling: Merging human variables and the social sciences with climate-glacier runoff models (Santa River, Peru). *J. Hydrol.* **2014**, *518*, 60–70. [CrossRef]

49. Van Leeuwen, W.J.D.; Hartfield, K.; Miranda, M.; Meza, F.J. Trends and ENSO/AAO driven variability in NDVI derived productivity and phenology alongside the Andes Mountains. *Remote Sens.* **2013**, *5*, 1177–1203. [CrossRef]

50. Panigada, C.; Tagliabue, G.; Zaady, E.; Rozenstein, O.; Garzonio, R.; Di Mauro, B.; De Amicis, M.; Colombo, R.; Cogliati, S.; Miglietta, F.; et al. A new approach for biocrust and vegetation monitoring in drylands using multi-temporal Sentinel-2 images. *Prog. Phys. Geogr.: Earth Environ.* **2019**, *43*, 496–520. [CrossRef]

51. Fensholt, R.; Horion, S.; Tagesson, T.; Ehammer, A.; Ivits, E.; Rasmussen, K. Global-scale mapping of changes in ecosystem functioning from earth observation-based trends in total and recurrent vegetation. *Glob. Ecol. Biogeogr.* **2015**, *24*, 1003–1017. [CrossRef]

52. Eastman, J.R.; Sangermano, F.; Ghimire, B.; Zhu, H.; Chen, H.; Neeti, N.; Cai, Y.; Machado, E.A.; Crema, S.C. Seasonal trend analysis of image time series. *Int. J. Remote Sens.* **2009**, *30*, 2721–2726. [CrossRef]

53. Verbesselt, J.; Hyndman, R.; Newnham, G.; Culvenor, D. Detecting trend and seasonal changes in satellite image time series. *Remote Sens. Environ.* **2010**, *114*, 106–115. [CrossRef]

54. Tote, C.; Beringhs, K.; Swinnen, E.; Govers, G. Monitoring environmental change in the Andes based on SPOT-VGT and NOAA-AVHRR time series analysis. In Proceedings of the 6th International Workshop on the Analysis of Multi-temporal Remote Sensing Images (IEEE 2011), Trento, Italy, 12–14 July 2011; pp. 268–272.

55. Zimmer, A.; Meneses, R.I.; Rabatel, A.; Soruco, A.; Dangles, O.; Anthelme, F. Time lag between glacial retreat and upward migration alters tropical alpine communities. *Perspect. Plant Ecol. Evolut. Syst.* **2018**, *30*, 89–102. [CrossRef]

56. Sugihara, G.; May, R.; Ye, H.; Hsieh, C.; Deyle, E.; Fogarty, M.; Munch, S. Detecting causality in complex ecosystems. *Science* **2012**, *338*, 496–500. [CrossRef] [PubMed]

57. Mainali, K.; Bewick, S.; Vecchio-Pagan, B.; Karig, D.; Fagan, W.F. Detecting interaction networks in the human microbiome with conditional Granger causality. *PLoS Comput. Biol.* **2019**, *15*, e1007037. [CrossRef]